THE JOURNAL OF BIOLOGICAL CHEMISTRY VOL. 286, NO. 11, pp. 9429–9442, March 18, 2011

Competitive Modulation of Ca^{2+} Release-activated Ca^{2+} Channel Gating by STIM1 and 2-Aminoethyldiphenyl Borate*[S]

Received for publication, October 8, 2010, and in revised form, December 3, 2010 Published, JBC Papers in Press, December 30, 2010, DOI 10.1074/jbc.M110.189035

Megumi Yamashita, Agila Somasundaram, and Murali Prakriya[1]

From the Department of Molecular Pharmacology and Biological Chemistry, Feinberg School of Medicine, Northwestern University, Chicago, Illinois 60611

Activation of Ca^{2+} release-activated Ca^{2+} channels by depletion of intracellular Ca^{2+} stores involves physical interactions between the endoplasmic reticulum Ca^{2+} sensor, STIM1, and the channels composed of Orai subunits. Recent studies indicate that the Orai3 subtype, in addition to being store-operated, is also activated in a store-independent manner by 2-aminoethyldiphenyl borate (2-APB), a small molecule with complex pharmacology. However, it is unknown whether the store-dependent and -independent activation modes of Orai3 channels operate independently or whether there is cross-talk between these activation states. Here we report that in addition to causing direct activation, 2-APB also regulates store-operated gating of Orai3 channels, causing potentiation at low doses and inhibition at high doses. Inhibition of store-operated gating by 2-APB was accompanied by the suppression of several modes of Orai3 channel regulation that depend on STIM1, suggesting that high doses of 2-APB interrupt STIM1-Orai3 coupling. Conversely, STIM1-bound Orai3 (and Orai1) channels resisted direct gating by high doses of 2-APB. The rate of direct 2-APB activation of Orai3 channels increased linearly with the degree of STIM1-Orai3 uncoupling, suggesting that 2-APB has to first disengage STIM1 before it can directly gate Orai3 channels. Collectively, our results indicate that the store-dependent and -independent modes of Ca^{2+} release-activated Ca^{2+} channel activation are mutually exclusive: channels bound to STIM1 resist 2-APB gating, whereas 2-APB antagonizes STIM1 gating.

Depletion of endoplasmic reticulum (ER)[2] Ca^{2+} stores following stimulation of cell surface receptors activates store-operated Ca^{2+} release-activated Ca^{2+} (CRAC) channels in many cells (1). The resulting Ca^{2+} influx regulates a wide array of cellular functions, including gene expression, motility, and the release of inflammatory mediators (2, 3). CRAC channels are encoded by three closely related proteins termed Orai1–3 (also known as CRACM1–3) (4–6), which assemble as homotetramers (7–9). Human patients bearing mutations that cause loss of Orai1 expression or channel function exhibit devastating immunodeficiencies, highlighting the importance of CRAC channels for immune host defense mechanisms (2, 10, 11).

Given their essential role in human immunity, CRAC channels have emerged as attractive candidates for the design of novel therapeutics to treat immune disorders such as chronic inflammation (11). However, selective modulators of CRAC channels are scarce, and the mechanism of action of many available modulators remains uncertain. One agent that has received widespread attention is the compound 2-APB (12). In native CRAC channels of T-cells, B-cells, and mast cells, 2-APB elicits complex effects, including a severalfold enhancement of I_{CRAC} at low concentrations (<5 μM) (termed potentiation) and transient potentiation followed by inhibition at high concentrations (>20 μM) (13, 14). 2-APB also reduces Ca^{2+}-dependent fast inactivation of I_{CRAC} in parallel with the slow development of its inhibitory effects at high concentrations (13). These effects are intriguing not only for the potential of 2-APB to be used as a basis for future drug development but also because modulation of key properties of CRAC channels such as activation and inactivation by 2-APB may be useful in understanding how these properties are controlled. Despite its widespread use in the Ca^{2+} signaling field, however, the molecular mechanisms of the various 2-APB effects on CRAC channels remain poorly understood.

When overexpressed with the ER Ca^{2+} sensor, STIM1, all three Orai proteins give rise to store-operated CRAC channels with broadly similar permeation and gating characteristics. These include high Ca^{2+} selectivity, low permeability to large monovalent cations such as Cs^{+}, and feedback inhibition by Ca^{2+} (15, 16). Store-dependent activation of all three isoforms arises from direct interaction of the channels with STIM1, which is redistributed from the bulk ER to peripheral ER regions in close proximity to the plasma membrane, thereby allowing direct binding to Orai channels in the plasma membrane (3). However, Orai1 and Orai3 have been reported to differ markedly in their regulation by 2-APB (17–21). Whereas Orai1 channels, like the endogenous CRAC channels in immune cells (13, 14), are transiently potentiated

* This work was supported, in whole or in part, by National Institutes of Health Grants NS057499 and GM082133 (to M. P.).

[S] The on-line version of this article (available at http://www.jbc.org) contains supplemental Figs. S1–S4.

[1] To whom correspondence should be addressed: Dept. of Molecular Pharmacology and Biological Chemistry, Northwestern University School of Medicine, 303 E. Chicago Ave., Ward 8-296, Chicago, IL 60611. Tel.: 312-503-7030; Fax: 312-503-5349; E-mail: m-prakriya@northwestern.edu.

[2] The abbreviations used are: ER, endoplasmic reticulum; CRAC, Ca^{2+} release-activated Ca^{2+}; 2-APB, 2-aminoethyldiphenyl borate; DVF, divalent ion-free; HEDTA, *N*-(2-hydroxyethyl) ethylenediaminetriacetic acid; TIRF, total internal reflection fluorescence; BAPTA, 1,2-bis(2-aminophenoxy)ethane-*N*,*N*,*N*′,*N*′-tetraacetic acid; TG, thapsigargin; CFP, cyan fluorescent protein; I, current; V, voltage.

and subsequently inhibited by high concentrations (>20 μM) of 2-APB (4, 17), Orai3 channels are strongly activated through a mechanism independent of ER Ca^{2+} stores and STIM1 (17–21). The 2-APB-activated Orai3 current also exhibits a significantly lower Ca^{2+} selectivity and higher Cs^{+} permeability than the STIM1-activated current (17–20).

These effects of 2-APB raise several questions regarding the mechanisms by which the compound regulates CRAC channel activity and the specificity of its effects for particular Orai isoforms. First, are there multiple mechanisms of 2-APB regulation of Orai3 channels? Previous reports have not differentiated the stimulation of Orai3 currents by low 2-APB doses from direct gating at high doses, instead implying that these effects occur through the same mechanism. Given that low doses of 2-APB potentiate native and Orai1 CRAC channels through a store-dependent mechanism, it is possible that the effects of low and high 2-APB doses on Orai3 channels arise through different mechanisms, but this has not been explored. Second, are store-operated Orai3 currents inhibited by high doses of 2-APB? Previous studies have shown that Orai1 and Orai2 channels are inhibited by high doses of 2-APB (17–19), but whether store-operated Orai3 currents are also inhibited by 2-APB is unknown (17–21). Third, is there positive or negative cross-talk between the store-dependent and -independent modes of regulation? Cross-talk could permit more finely tuned regulation of CRAC channel activity than that achievable by the independent action of each gating mode. Given recent findings indicating that CRAC channels can be activated by endogenous factors in a store-independent manner (22), elucidation of potential cross-talk is directly relevant for a better understanding of the mechanisms controlling CRAC channel activity.

To address these issues, we studied the effects of 2-APB on store-operated and store-independent modes of activation of Orai3 and Orai1 CRAC channels. We found that in addition to store-independent activation 2-APB elicited a range of other effects on Orai3 channels, including STIM1-dependent potentiation at low concentrations (<10 μM) and persistent inhibition of the store-operated current at high concentrations (>20 μM). Thus, the key effects of 2-APB seen in Orai1 and native CRAC currents also occur in store-operated Orai3 channels. Inhibition of Orai3 current by high doses of 2-APB was accompanied by elimination of STIM1-dependent fast inactivation and low dose potentiation, suggesting that 2-APB causes functional uncoupling of STIM1 from Orai3 channels. Importantly, our results indicate that Orai3 channels bound to STIM1 resist 2-APB gating, whereas 2-APB suppresses STIM1 gating. Thus, the STIM1-dependent and 2-APB-dependent activation states of Orai3 channels do not co-exist but are mutually exclusive.

EXPERIMENTAL PROCEDURES

Cells—HEK293 cells were maintained in suspension in a medium containing CD293 supplemented with 4 mM GlutaMAX (both from Invitrogen) at 37 °C and 5% CO_2. To prepare them for imaging and electrophysiology, cells were plated and adhered to poly-L-lysine-coated coverslips at the time of passage and grown for 24 h. Cells were transfected in a medium containing 44% DMEM (Mediatech), 44% Ham's F-12 (Mediatech), 10% fetal calf serum (HyClone), 2 mM glutamine, 50 units/ml penicillin, and 50 μg/ml streptomycin.

Plasmids and Transfections—Two CFP-Orai3 constructs obtained from Drs. Jim Putney (NIEHS, Research Triangle Park, NC) (18) and Christoph Romanin (University of Linz) (20) were used in this study. The electrophysiology reported here was performed using the construct obtained from Dr. Putney except for studies on L285D Orai3 and corresponding controls, which were performed using the construct from Dr. Christoph Romanin (University of Linz). No systematic differences were noted between the two constructs. All imaging data reported here are from the Romanin laboratory construct. The IRES-eGFP-Orai1 plasmid has been described previously (23, 24). Unlabeled STIM1 for the electrophysiology was obtained from Origene Technologies (Rockville, MD). The STIM1-YFP plasmid has been described previously (25). Site-directed mutagenesis to generate Orai3 and Orai1 mutants was performed using the QuikChange™ site-directed mutagenesis kit (Stratagene) according to the manufacturer's instructions. siSTIM1 was obtained from Ambion. Cells were transfected with the indicated constructs using Transpass D2 (New England Biolabs) or Lipofectamine (Invitrogen) according to the manufacturer's instructions and studied 24 h later. Cells transfected with siSTIM1 were studied 48–72 post-transfection.

Solutions and Chemicals—The standard extracellular Ringer's solution contained 135 mM NaCl, 4.5 mM KCl, 20 mM $CaCl_2$, 1 mM $MgCl_2$, 10 mM D-glucose, and 5 mM Na-Hepes (pH 7.4). The 110 mM Ca^{2+} solution contained 110 mM $CaCl_2$, 10 mM D-glucose, and 5 mM Hepes (pH 7.4). The divalent ion-free (DVF) Ringer's solution contained 150 mM NaCl, 10 mM HEDTA, 1 mM EDTA, and 10 mM Hepes (pH 7.4). For the FRET and TIRF experiments, the extracellular solution contained 150 mM NaCl, 4.5 mM KCl, 2 mM $CaCl_2$, 1 mM $MgCl_2$, 10 mM D-glucose, and 5 mM Na-Hepes (pH 7.4). For the Ca^{2+}-free Ringer's solution, $CaCl_2$ was omitted from this solution, and the $MgCl_2$ concentration was increased to 3 mM. pH was adjusted to 7.4 with NaOH. 10 mM tetraethylammonium chloride was added to all extracellular solutions used for electrophysiology to prevent contamination from voltage-gated K^{+} channels. The standard internal solution contained 135 mM cesium aspartate, 8 mM $MgCl_2$, 8 mM BAPTA, and 10 mM Cs-Hepes (pH 7.2). Stock solutions of thapsigargin (Sigma) and 2-APB (Sigma) were prepared in DMSO at concentrations of 1 and 100 mM, respectively. Solutions were applied using a multibarrel local perfusion pipette with a common delivery port. Reversal potential measurements with 150 mM extracellular KCl applications indicated that the solution exchange time was <1 s.

Patch Clamp Measurements—Patch clamp recordings were performed using an Axopatch 200B amplifier (Axon Instruments, Foster City, CA) interfaced to an ITC-18 input/output board (Instrutech, Port Washington, NY) and an iMac G5 computer. Currents were sampled at 5 kHz and filtered at 1 kHz with a four-pole Bessel filter. Stimulation, data acquisition, and analysis were performed using routines developed on the Igor Pro platform (Wavemetrics, Lake Oswego, OR).

Data are corrected for the liquid junction potential of the pipette solution relative to Ringer's solution in the bath (−10 mV). The holding potential was +30 mV. The standard voltage stimulus consisted of a 100-ms step to −100 mV followed by a 100-ms ramp from −100 to +100 mV applied at 1-s intervals. For examining Ca^{2+}-dependent fast inactivation, the voltage protocol consisted of a 300-ms step to −100 mV followed by a 100-ms ramp from −100 to +100 mV applied at 1-s intervals. Unless otherwise indicated, cells were usually pretreated with 1 μM thapsigargin (TG) prior to establishment of the seal to deplete stores and activate CRAC channels.

FRET Microscopy—HEK293 cells were plated onto poly-L-lysine-coated coverslip chambers and imaged either with epifluorescence or with through-the-objective TIRF microscopy on an IX71 inverted microscope (Olympus, Center Valley, PA). For epifluorescence FRET microscopy, cells were imaged with a 60× oil immersion objective (UPlanApo; numerical aperture, 1.40), a 175-watt xenon arc lamp (Sutter, Novato, CA), and excitation and emission filter wheels (Sutter) as described previously (25). At each time point, three sets of images (CFP, YFP, and FRET) were captured on a cooled charge-coupled device camera (Hamamatsu, Bridgewater, NJ) using the following filters (Chroma Technology): CFP (I_{DD} image): excitation, 440 ± 20 nm; dichroic, Z458/514RPC; and emission, 485 ± 30 nm; YFP (I_{AA} image): excitation, 500 ± 20 nm; dichroic, Z458/514RPC; and emission, 535 ± 30 nm; and FRET (I_{DA} image): excitation, 440 ± 20 nm; dichroic, Z458/514RPC; and emission, 535 ± 30 nm. Image acquisition and analysis were performed with Slidebook software (Imaging Innovations Inc., Denver, CO). Images were captured at 12-s intervals at an exposure of 200 ms with 2 × 2 binning. Lamp output was attenuated to 25% by a 0.6 neutral density filter in the light path to minimize photobleaching. All experiments were performed at room temperature.

FRET analysis was performed using the E-FRET method described by Zal and Gascoigne (26). Bleed-through factors ($a = 0.09$, $b = 0.008$, $c = 0.002$, and $d = 0.33$) were determined as described previously (25). The apparent FRET efficiency was calculated from background-subtracted images using the formula (26)

$$E_{app} = \frac{F_c}{F_c + GI_{DD}} \quad \text{(Eq. 1)}$$

where $F_c = I_{DA} - aI_{AA} - dI_{DD}$. The instrument-dependent G factor was determined as described previously (25) and had the value 2.7 ± 0.2.

TIRF Microscopy—HEK293 cells expressing CFP-Orai3 and/or STIM1-YFP were illuminated by laser output from an argon ion laser (Melles Griot, Carlsbad, CA; 457–514-nm output) coupled to an illuminator that focused light on the back focal plane of a TIRF objective (PlanApo 60×, 1.45 numerical aperture, Olympus). TIRF illumination was achieved by controlling the position of a translatable prism to alter the incident angle of the laser beam. CFP, YFP, and FRET images were collected using the following combinations of filters and dichroics (Chroma): CFP: excitation, ET458 ± 10 nm; dichroic, Z458/514RPC; emission, ET485/30; YFP: excitation, ET514 ± 10 nm; dichroic, Z458/514RPC; emission, ET550 ± 50 nm; FRET: excitation, ET458 ± 10 nm; dichroic, Z458/514RPC; emission, ET514 ± 10 nm. Images were captured at 7-s intervals at an exposure of 500 ms (CFP image), 400 ms (YFP image), and 500 ms (FRET image) with 2 × 2 pixel binning. Bleed-through factors for computing E-FRET were as follows: $a = 005$ and $d = 0.58$.

Analysis of Patch Clamp Data—All current traces were corrected for leak currents collected in 20 mM Ca^{2+} + 20–50 μM La^{3+}. Averaged results are presented as the mean value ± S.E. The latency of current activation by 2-APB was measured by detecting the time point at which the current amplitude increased by 3 standard deviations beyond the base-line current. Base-line current was defined as the mean current during 15 s preceding the application of the drug. Rise time was quantified by measuring the time taken for the current to increase from the 10 to 90% value following 2-APB application.

RESULTS

Previous studies have described the direct activation of a non-selective Orai3 conductance by high concentrations of 2-APB (17–20). In the present study, our aim was to investigate whether 2-APB additionally modulates the store-operated gating mode of Orai3 channels and determine whether there is cross-talk between the STIM1-dependent and -independent activities of Orai3 channels. For most of the experiments described here, an N-terminally tagged Orai3 (CFP-Orai3) was expressed in HEK293 cells either together with unlabeled STIM1 or alone, and the functional effects of 2-APB were evaluated by patch clamp electrophysiology. Co-expression of CFP-Orai3 and STIM1 in HEK293 cells resulted in currents with several typical characteristics of store-operated Orai3 channels. These characteristics included an inwardly rectifying current-voltage relationship lacking a clear reversal potential in 20 mM $Ca^{2+}{}_o$, gradual decay (depotentiation) of the Na^+ current in DVF solution, a reversal potential of ~+50 mV in DVF solution indicating low permeability to intracellular Cs^+, and Ca^{2+}-dependent fast inactivation (supplemental Fig. S1).

Low Concentrations of 2-APB Potentiate Orai3 Currents in Store- and STIM1-dependent Manner—Low concentrations of 2-APB (1–10 μM) enhance CRAC channel activity in T-cells, B-cells, and mast cells, an effect termed potentiation (13, 14). Unlike the store-independent, direct activation of Orai3 channels by high doses of 2-APB described recently (17–20), potentiation occurs only after store depletion and without changes in ion selectivity (13, 14). Likewise, low doses of 2-APB also potentiate exogenously expressed Orai1 CRAC channels (4). Whether Orai3 channels can be similarly potentiated remains uncertain. Some recent studies have described current enhancement at low doses of 2-APB (<20 μM) (17–20) but have not differentiated this effect from the direct activation of the non-selective Orai3 current by high doses of 2-APB (>40 μM).

To examine this issue directly, we investigated the effects of low doses of 2-APB on store-operated Orai3 currents. Application of a low concentration of 2-APB (5 μM) to store-de-

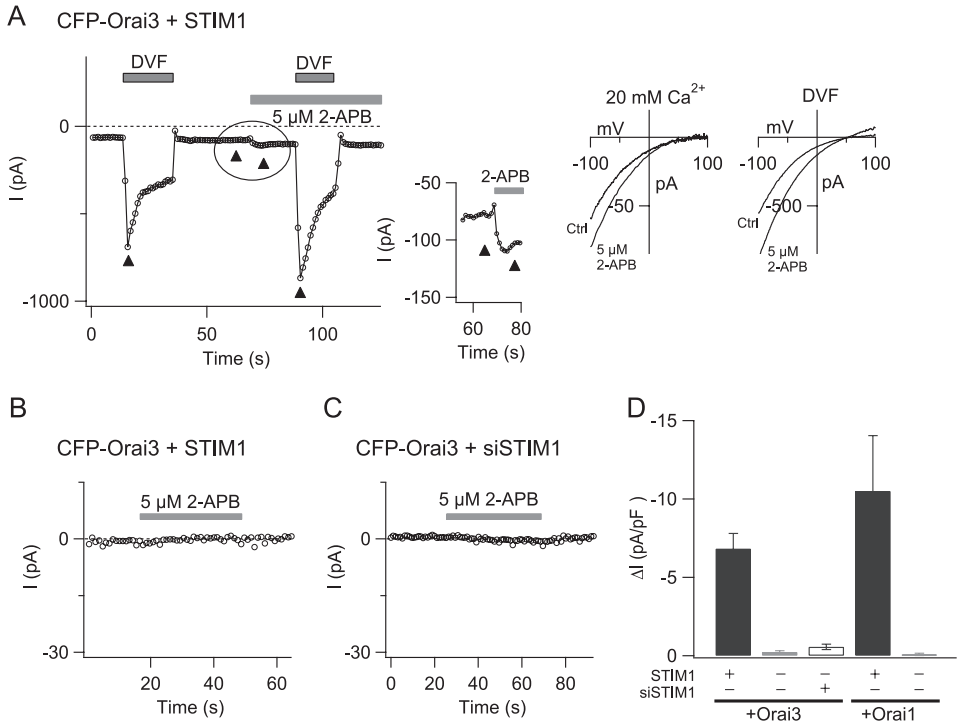

FIGURE 1. **Low concentrations of 2-APB potentiate Orai3 channels in STIM1-dependent manner.** *A*, a low concentration of 2-APB (5 μM) was applied to a TG-treated HEK293 cell co-expressing CFP-Orai3 and STIM1. Leak-corrected peak currents during hyperpolarizing steps to −100 mV are plotted against time as the extracellular solution was changed from 20 mM Ca^{2+}_o to a DVF solution. The *inset* shows the stimulation of Orai3 I_{CRAC} caused by 2-APB. The ramp I-Vs shown in the *right* graphs were recorded at the time points indicated by the *arrowheads* in the *left* graphs. *B*, a low dose of 2-APB (5 μM) does not stimulate I_{CRAC} in resting cells with replete stores. This cell was transfected with CFP-Orai3 and STIM1. [Ca^{2+}] in the pipette solution was buffered to 100 nM to prevent store depletion and passive activation of I_{CRAC}. *C*, potentiation is lost in cells treated with siSTIM1. Cells were transfected with CFP-Orai3 and siSTIM1, and currents were recorded in TG-treated cells 48–72 h later. Store-operated Ca^{2+} entry was suppressed by ~50% in HEK293 cells transfected with siSTIM1 alone (data not shown). *D*, summary of the potentiating effects of 5 μM 2-APB on Orai3 and Orai1 channels in cells overexpressing STIM1, in cells expressing no exogenous STIM1, and in cells treated with siSTIM1 (n = 4–9 cells). Data are represented as mean ± S.E. Because there is little or no store-operated current in the absence of STIM1 expression, potentiation was quantified as the increase in current amplitude (normalized to the cell capacitance) caused by 5 μM 2-APB. *Ctrl*, control; *pF*, picofarad.

pleted cells enhanced the inward current (Fig. 1*A*). The current-voltage (I-V) relationship of the 2-APB-stimulated current resembled Orai3 I_{CRAC} (Fig. 1*A*), indicating that the ion selectivity of the 2-APB-stimulated current is unchanged. Importantly, enhancement of Orai3 I_{CRAC} by low doses of 2-APB required depletion of intracellular Ca^{2+} stores. Application of 2-APB (5 μM) on resting cells with intracellular [Ca^{2+}] buffered to 100 nM had no effect, indicating that rather than directly activating Orai3 I_{CRAC}, low doses of 2-APB boost activity of Orai3 channels following activation by store depletion (Fig. 1*B*). In support of this interpretation, potentiation of Orai3 I_{CRAC} required exogenously expressed STIM1. Potentiation was significantly reduced in cells transfected with Orai3 alone and in cells treated with siSTIM1 (Fig. 1, *C* and *D*). Similar results were seen in cells transfected with Orai1 alone (Fig. 1*D* and supplemental Fig. S2). Collectively, these results argue that low doses of 2-APB potentiate Orai3 currents in an ER Ca^{2+} store- and STIM1-dependent manner without eliciting major changes in the properties of the current, reminiscent of potentiation seen in native CRAC channels and in Orai1-encoded CRAC channels.

High Concentrations of 2-APB Inhibit Store-operated Orai3 CRAC Currents—In immune cells, a high dose of 2-APB transiently potentiates I_{CRAC} and over longer durations produces strong inhibition that is poorly reversed by washout of the compound (13). Likewise, high doses of 2-APB strongly and persistently inhibit exogenously expressed Orai1 and Orai2 currents (17–20). An example of this well described effect is illustrated for Orai1 in supplemental Fig. S2C. However, whether store-operated Orai3 channels are also inhibited by high concentrations of 2-APB is unclear. Previous studies have argued that, in contrast to Orai1 channels and CRAC channels of T-cells, B-cells, and mast cells, 2-APB only facilitates Orai3 currents (17–20). Nevertheless, the ability of 2-APB to powerfully activate Orai3 channels directly in a store-independent fashion could have masked inhibition of store-operated gating.

To address this issue, we exploited the fact that inhibition of Orai1 CRAC current by 2-APB persists following washout of the compound. Hence, comparison of current amplitudes prior to the application of 2-APB and following its washout offers a straightforward method to test whether the drug also inhibits store-operated Orai3 current. Indeed, this method revealed strong suppression of the store-operated Orai3 conductance (81 ± 3% inhibition; 50 μM 2-APB applied for 100 s; n = 5) (Fig. 2*A*). Inhibition of the store-operated conductance was specific to high concentrations of 2-APB (>20 μM). Lower concentrations of 2-APB (5–10 μM) that potentiated Orai3 CRAC currents did not elicit the long lasting current inhibition (supplemental Fig. S1D). Suppression of the store-

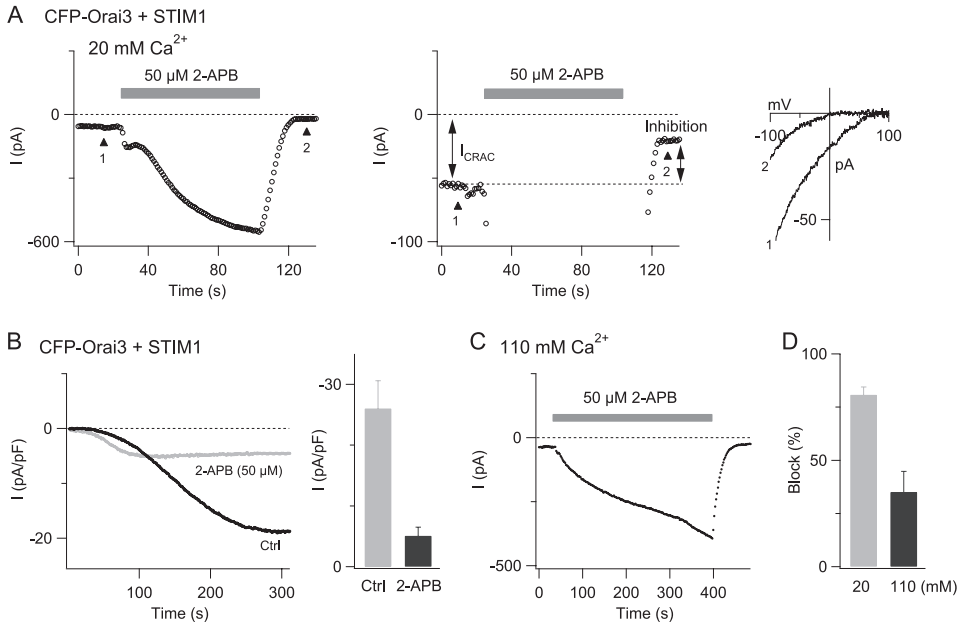

FIGURE 2. **High concentrations of 2-APB inhibit store-operated Orai3 currents.** *A*, a cell overexpressing CFP-Orai3 and STIM1 was pretreated with 1 μM TG before patch clamp recording. The *left* graph shows the steady-state current at −100 mV at a low gain to illustrate the large degree of direct activation of Orai3 channels by 50 μM 2-APB. The *right* graph shows the same experiment at a high gain to visualize effects on the store-operated Orai3 current before and after washout of 2-APB. Ramp I-Vs collected at the time points indicated by the *arrowheads* are shown in the *rightmost* graph. *B*, a resting HEK293 cell co-expressing CFP-Orai3 and STIM1 was exposed to 50 μM 2-APB. Following washout of 2-APB, the cell was patched, and I_{CRAC} activation was monitored during passive depletion of ER Ca^{2+} stores with 8 mM BAPTA. The *left* graph plots the time course of the current in a control cell (*black* trace) and a cell pretreated with 2-APB (*gray* trace). The bar graph on the *right* summarizes the steady-state current densities from four to five cells. *C*, 2-APB-mediated inhibition of the store-operated conductance is reduced in the presence of 110 mM Ca^{2+}_o. 2-APB (50 μM) was applied as described above on a store-depleted cell co-expressing CFP-Orai3 and STIM1. *D*, summary of the 2-APB-mediated inhibition of store-operated Orai3 currents in 20 and 110 mM Ca^{2+}_o. *Ctrl*, control; *pF*, picofarad.

operated Orai3 current by high concentrations of 2-APB (50 μM) also occurred when the drug was applied in a Ca^{2+}-free solution (65 ± 3% inhibition in 0 Ca^{2+} + 3 mM Mg^{2+}; $n = 3$ cells). Thus, the inhibition observed when 2-APB was applied in the presence of extracellular Ca^{2+} is not simply due to inactivation by high $[Ca^{2+}]_i$ caused by direct Orai3 channel activation.

In the above experiments, 2-APB was applied to store-depleted cells with activated CRAC channels. To test whether 2-APB inhibition is also observed if the drug is applied prior to store depletion, we pretreated resting cells with 50 μM 2-APB for 5–10 min. Then, following washout of the drug with Ringer's solution, we patched the 2-APB-exposed cells and measured the amplitude of the store-operated Orai3 current activated by passive store depletion with 8 mM BAPTA. This protocol also resulted in significant suppression of store-operated Orai3 current (Fig. 2*B*). Because 2-APB was applied prior to depletion of intracellular stores, this result suggests that the observed inhibition likely arises because of attenuation of the upstream activation mechanism rather than simple pore occlusion. It also indicates that the inhibition seen in Fig. 2*A* is due to specific suppression of store-operated gating and not merely due to nonspecific rundown or washout of obligatory intracellular components during the whole-cell recording. Collectively, these results indicate that as previously seen in Orai1 and native CRAC channels, high concentrations of 2-APB inhibit store-operated Orai3 CRAC currents. 2-APB inhibition in Orai1 and native CRAC currents differs from Orai3 channels in that in the former cases inhibition is readily visible during the application of the compound, whereas because of the strong direct activation of Orai3 channels by 2-APB, inhibition of store-operated gating is revealed clearly only following washout of the compound.

The degree of inhibition of the store-operated conductance depended on the concentration of the permeant ion. When the extracellular Ca^{2+} concentration was raised from 20 to 110 mM, inhibition of the store-operated conductance was greatly reduced (Fig. 2, *C* and *D*). We did not further probe the underlying mechanisms of this effect but as described later, we exploited this phenomenon to probe the relationship between the 2-APB inhibition of the store-operated current and direct activation of the non-selective current by high doses of 2-APB.

Delayed Activation of Outward Currents by High Doses of 2-APB—As described in several previous studies (17–20), high doses of 2-APB produce large, store-independent Orai3 currents in cells co-expressing Orai3 and STIM1 (*e.g.* Fig. 2*A*). At steady state, the large currents activated by 2-APB are outwardly rectifying and exhibit reduced Ca^{2+} selectivity and increased Cs^+ permeability (supplemental Fig. 1C) (17–20). Although these steady-state conduction properties are well described, less is known about the kinetics of current activation by 2-APB. In fact, we found that following exposure to 2-APB (50 μM) the inward current (at −100 mV) did not increase with monotonic kinetics but instead displayed a biphasic time course (Fig. 3*A*). The first phase consisted of a rapid increase that plateaued in 10–20 s. This was followed by a large, secondary enhancement that occurred over tens of sec-

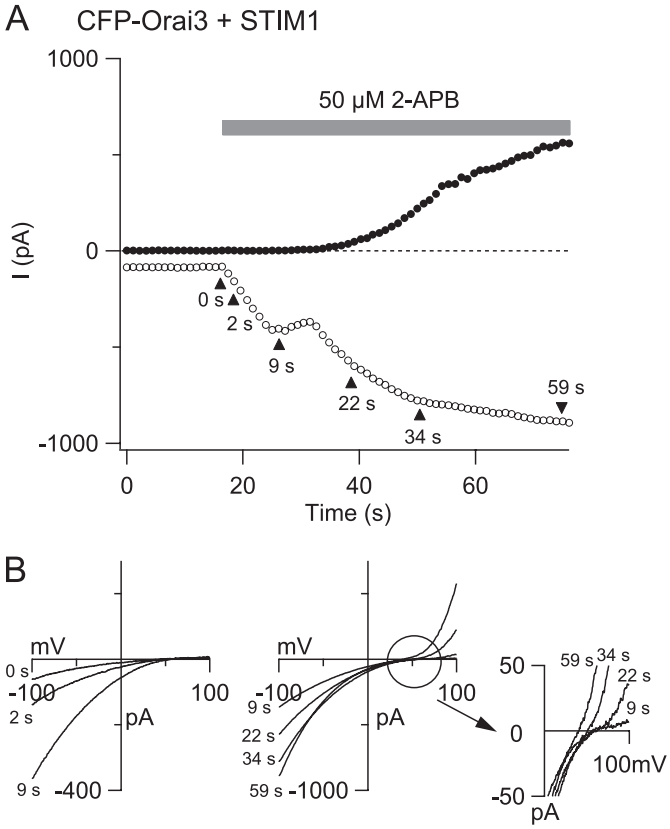

FIGURE 3. **Delayed activation of non-selective Orai3 current by high doses of 2-APB in STIM1-overexpressing cells.** *A*, a TG-treated cell overexpressing CFP-Orai3 and STIM1 was exposed to 50 μM 2-APB. Leak-corrected currents at −100 mV (*open circles*) and +100 mV (*closed circles*) collected from ramp I-Vs are plotted against time. *B*, the graphs show the ramp I-Vs collected at the time points indicated by the *arrowheads* in *A*. The *left* graph plots the increase in I_{CRAC}-like current during the first phase of current stimulation, whereas the *right* graph depicts the current enhancement during the second phase. The development of the outward current is accompanied by a progressive shift in the reversal potential of the current (shown in the *inset*).

onds. The current-voltage relationship of the early phase exhibited the classical inward rectification of store-operated I_{CRAC} (Fig. 3*B*). Only after a latency of 14 ± 2 s (n = 7 cells) was activation of the outward current detected (Fig. 3*B*). Thus, in cells co-expressing Orai3 and STIM1, the inward and outward currents are activated with markedly distinct kinetics.

The differences in the activation kinetics of the inward and outward currents and alterations in ion selectivity were most clearly revealed as the drug concentration was progressively increased in the same cell. In the example shown in supplemental Fig. S3, increasing 2-APB concentration from 10 to 20 μM and finally 50 μM resulted in the slow appearance of outward currents and a leftward shift in the reversal potential. These results indicate that at high doses 2-APB elicits at least two kinetically distinct effects on Orai3 channels consisting of an initial increase in Orai3 I_{CRAC} with no detectable change in ion selectivity followed by secondary activation of Orai3 channels with altered ion selectivity.

STIM1 Delays Direct Activation of Orai3 Currents by High Doses of 2-APB—The biphasic current activation by high doses of 2-APB could represent progression of a single store-independent gating process as suggested previously (17, 18) or alternately indicate the presence of two distinct gating processes. A simple possibility is that the initial stimulation of Orai3 currents with characteristic hallmarks of I_{CRAC} arises due to potentiation of the store-operated Orai3 I_{CRAC}, whereas the latter phase arises from direct, store-independent activation of the non-selective Orai3 current. To test this, we examined currents activated by 2-APB in cells expressing CFP-Orai3 alone (*i.e.* without exogenous STIM1). We reasoned that, because potentiation is STIM1-dependent (Fig. 1*D*), the initial stimulation of inward current with characteristic I_{CRAC}-like features would be diminished in cells expressing CFP-Orai3 alone where channels are predicted to be free of STIM1.

Before testing this hypothesis, we sought assurance that Orai3 channels in cells expressing CFP-Orai3 alone are functionally "free" of STIM1. We tested this in two ways. First, we compared the distribution of Orai3 channels in cells expressing CFP-Orai3 alone and in cells co-expressing CFP-Orai3 and STIM1-YFP. Consistent with the abundance of literature indicating that store-dependent activation of Orai channels involves direct interactions with STIM1 at the ER-plasma membrane junctions (27–31), depletion of intracellular Ca^{2+} stores in cells co-expressing CFP-Orai3 and STIM1 resulted in aggregation of Orai3 and STIM1 into overlapping puncta and increases in Orai3-STIM1 FRET (Fig. 4*A*). By contrast, in cells expressing CFP-Orai3 alone, Orai3 fluorescence in the plasma membrane remained diffuse following depletion of intracellular Ca^{2+} stores (Fig. 4*B*). Because STIM1-bound Orai channels are expected to be recruited to puncta, this result suggests that Orai3 channels in these cells have insufficient STIM1 for punctum formation. In a second test, we examined whether the Orai3 current activated by 2-APB displays Ca^{2+}-dependent fast inactivation (Fig. 4*C*). Recent evidence indicates that STIM1 is essential for fast inactivation, and an acidic amino acid-rich region in the C terminus of STIM1 is essential for this process (32–34). In cells expressing Orai3 alone, store-operated currents were not detected. Moreover, in contrast to the store-operated current in cells expressing CFP-Orai3 and STIM1, the 2-APB-activated Orai3 current completely lacked fast inactivation (Fig. 4*C*) (supplemental Fig. S1A). Taken together, these results indicate that there is stoichiometrically insufficient STIM1 in cells transfected with Orai3 alone for store-dependent activation, punctum formation, and fast inactivation.

Next, we explored the effects of 2-APB on the STIM1-free Orai3 channels. 2-APB (50 μM) did not cause visible changes in the pattern of localization of CFP-Orai3 (Fig. 4*B*), indicating that, unlike the STIM1-mediated activation of Orai3 channels, store-independent activation by 2-APB occurs without clustering of channels into puncta. Application of 50 μM 2-APB to cells expressing CFP-Orai3 alone resulted in activation of Orai3 currents with biophysical properties closely resembling the steady-state 2-APB-activated currents in cells co-expressing Orai3 and STIM1 (Fig. 5*A*). The reversal potentials of currents in 20 mM $Ca^{2+}{}_o$ and DVF solutions following 200-s exposures to 50 μM 2-APB were similar between cells co-expressing CFP-Orai3 and STIM1 and cells expressing

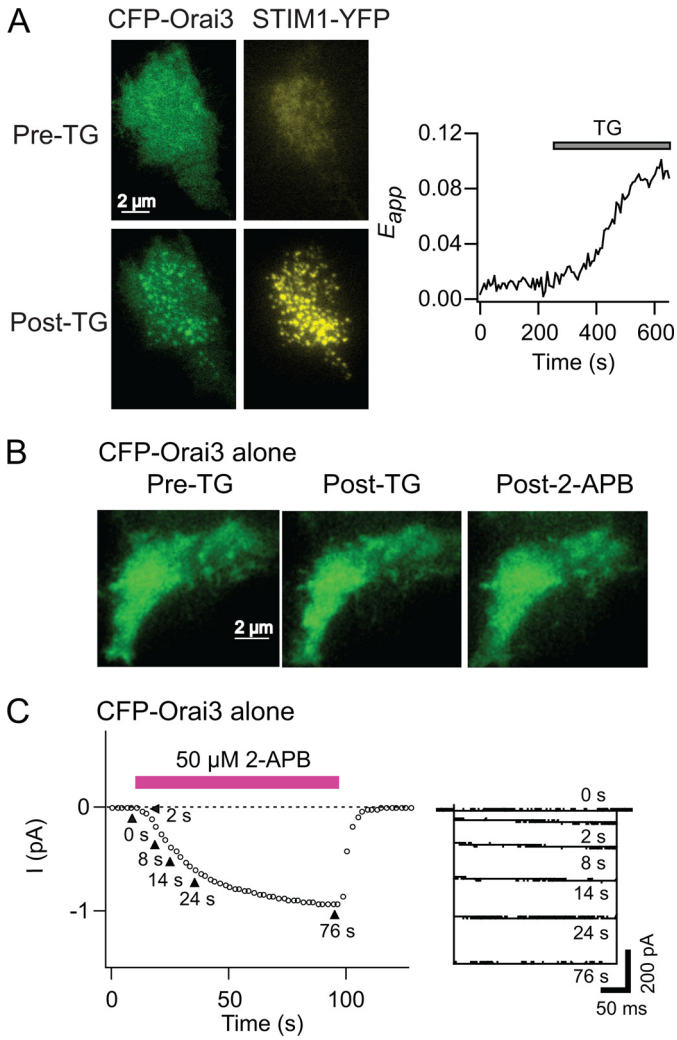

FIGURE 4. **Orai3 channels in cells expressing CFP-Orai3 alone are functionally free of STIM1.** *A*, an HEK293 cell co-expressing CFP-Orai3 and STIM1-YFP was imaged using TIRF microscopy. Selected images from a time lapse run in 2 mM Ca^{2+} (*Pre-TG*) and 480 s following the addition of 1 μM TG (*Post-TG*) are illustrated. The *right* graph plots the increase in E-FRET in the same cell in response to store depletion. *B*, a cell overexpressing CFP-Orai3 alone (but not STIM1) was imaged using TIRF microscopy. The cell was exposed to TG (1 μM) and 10 min later to 2-APB (50 μM). The cell shown is representative of seven cells. *C*, 2-APB-gated Orai3 currents do not exhibit fast inactivation. 50 μM 2-APB was applied to a cell expressing CFP-Orai3 alone (no STIM1). The membrane was hyperpolarized to −100 mV (300 ms) at 1-s intervals, and the 2-APB-activated current at −100 mV was plotted against time. The traces on the *right* show the current responses at the time points indicated in the *left* graph.

CFP-Orai3 alone (33 ± 1 and 2 ± 2 mV, $n = 13$ cells and 30 ± 2 and 5 ± 1 mV, $n = 6$ cells, respectively). Moreover, the maximal 2-APB-activated current amplitudes (during 200–300-s applications of 2-APB) in STIM1- and Orai3-co-expressing cells were similar to those in cells expressing Orai3 alone (supplemental Fig. S4A).

Despite these similarities in steady-state properties, the kinetics of the 2-APB-activated current differed in two major respects between cells expressing Orai3 alone and the STIM1-co-expressing cells. First, potentiation of the inward current was eliminated in cells expressing Orai3 alone, and in its absence, activation of inward and outward currents occurred with very similar time courses (Fig. 5*A*). As a result, the 2-APB-stimulated current exhibited a constant reversal potential with gradually increasing amplitude (contrast the progressive leftward shift in reversal potential seen in Fig. 3*B* with the constant reversal potential seen in Fig. 5*A*). Second, store-independent activation of the non-selective current occurred with dramatically faster kinetics in cells expressing Orai3 alone. This was most clearly manifested in the latency of outward current activation, which was significantly shorter in cells expressing Orai3 alone (Fig. 5*C*). Because the outward current is an unambiguous manifestation of direct activation of Orai3 channels by 2-APB, this result indicates that the long delay in direct activation in cells co-expressing Orai3 and STIM1 is caused by the presence of STIM1.

In addition to accelerated latency, the rate of current increase as measured by the 10–90% rise time was also considerably faster in cells expressing Orai3 alone (Fig. 5*D*). Rise time measurements were complicated by the complex kinetics of the 2-APB-activated current, which often exhibited slow attenuation during prolonged drug applications (>100 s). Although the extent of slow inhibition was variable, it was observed both in cells expressing CFP-Orai3 alone and when CFP-Orai3 and STIM1 were co-expressed. Preliminary studies indicate that the slow decline following maximal activation of the 2-APB-stimulated current is likely driven by feedback inhibition by $[Ca^{2+}]_i$ elevations,[3] and further experiments are in progress to confirm this hypothesis. Nevertheless, the faster activation kinetics in cells expressing Orai3 alone is consistent with the conclusion that STIM1 delays direct activation of Orai3 channels. Together with the shorter latency of current activation described above, these results argue that Orai3 channels in store-depleted cells co-expressing STIM1 and Orai3 are resistant to direct activation by 2-APB.

Resistance to 2-APB Activation Requires STIM1-Orai3 Binding—To test whether the delay in the 2-APB-mediated activation is simply an effect of STIM1 overexpression or specifically requires STIM1-Orai3 interaction, we examined the effects of 50 μM 2-APB in an Orai3 mutant with impaired STIM1 binding. A putative coiled coil domain in the C terminus of Orai1 is critical for CRAC channel activation by STIM1, and mutations of conserved hydrophobic residues within this region interfere with STIM1 binding (35). In particular, the L276D Orai1 mutation disrupts channel interaction with STIM1 and fails to produce store-operated CRAC currents (25). Likewise, we found that the equivalent mutation in Orai3 (L285D) eliminated punctum formation of L285D Orai3 channels, abolished increases in STIM1-Orai3 FRET, and diminished the store-operated Orai3 current by ~90% (Fig. 6, *A* and *B*, and supplemental Fig. S4B). High doses of 2-APB directly activated a non-selective conductance in this mutant with steady-state current amplitudes similar to those of WT Orai3 (supplemental Fig. S4A). However, despite co-expression of STIM1, the latency and rise time of 2-APB-activated currents in L285D Orai3 was significantly faster than those seen in cells co-expressing WT CFP-Orai3 and STIM1 and instead resembled the behavior seen in cells ex-

[3] M. Yamashita and M. Prakriya, unpublished data.

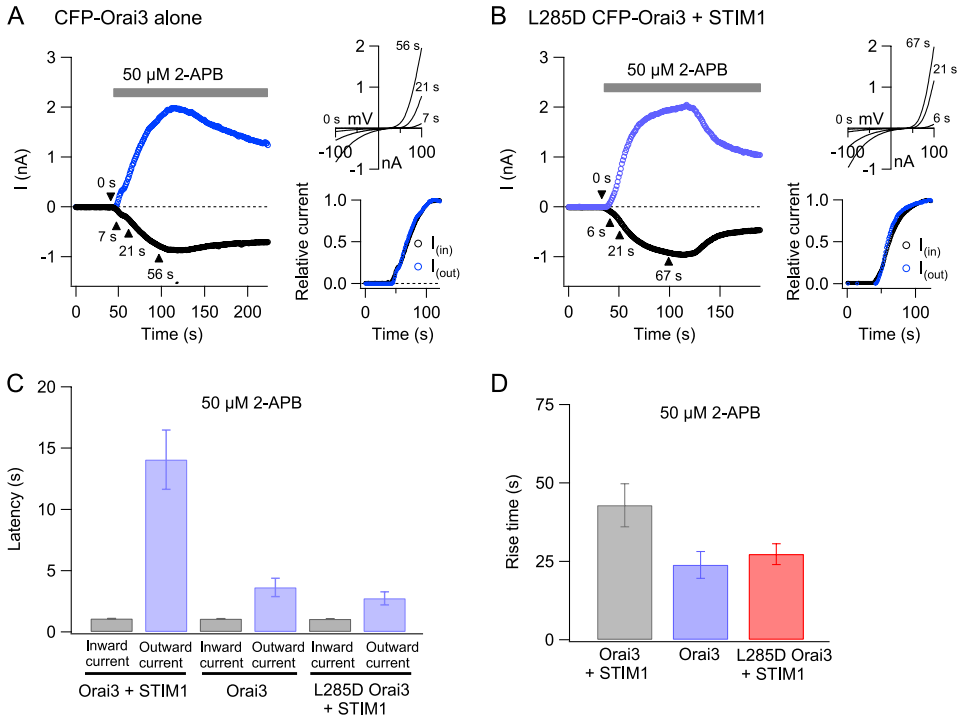

FIGURE 5. **Direct activation of Orai3 current by 2-APB is accelerated in absence of STIM1.** *A*, the *left* graph shows currents at −100 and +100 mV (*black* and *blue* traces, respectively) activated by a high concentration of 2-APB (50 μM) in a cell overexpressing CFP-Orai3 alone. The same currents are plotted on a normalized *y axis* scale in the *right lower* graph. Ramp I-Vs collected at the indicated time points are also shown. *B*, the kinetics of inward and outward currents (*black* and *blue* traces, respectively) in a cell co-expressing L285D Orai3 and STIM1. *C*, summary of the latency of current activation under various conditions. The latency of activation of the outward current was measured as described under "Experimental Procedures." *D*, the 10–90% rise time of the outward Orai3 current (at +100 mV) in the three groups of cells. In all cases, cells were pretreated with TG to deplete stores.

pressing Orai3 alone (Fig. 5, *B–D*). These results argue that a physical interaction with STIM1 is required for resistance to direct 2-APB gating.

STIM1-bound Orai1 Channels Also Resist 2-APB Activation—We found that the inhibitory influence of STIM1 on direct activation by high concentrations of 2-APB was not unique to Orai3 channels but also occurred in Orai1 CRAC channels. In cells co-expressing Orai1 and STIM1, application of a high concentration of 2-APB (50 μM) for 40–60 s did not result in direct activation in all cells tested (supplemental Fig. S2C). Rather, only potentiation followed by slow inhibition of the store-operated Orai1 current was observed in these cells (supplemental Fig. S2C). By contrast, application of 50 μM 2-APB for 40–60 s to cells overexpressing Orai1 alone led to the development of an outwardly rectifying current with an I-V relationship resembling the 2-APB-activated Orai3 current in all cells tested (seven of seven) as described previously (17) (Fig. 7, *A* and *B*). Amplitudes of 2-APB-activated Orai1 currents were generally smaller than those seen in Orai3 channels (Orai1: current density at +100 mV, 8.4 ± 0.4 pA/picofarad; $n = 7$; Orai3: 131.9 ± 39.7 pA/picofarad; $n = 6$). Thus, STIM1-bound Orai1 channels are also resistant to direct activation by 2-APB.

2-APB Causes Functional Uncoupling of STIM1 from Orai3 Channels—We next probed the mechanisms of inhibition of the store-operated Orai3 I_{CRAC} by high doses of 2-APB. In Orai1 channels, some reports have suggested that 2-APB inhibition of the store-operated current is mediated by disruption of STIM1-Orai1 coupling (17, 18). This conclusion was derived from observations that high doses of 2-APB reverse STIM1 puncta (17, 18). However, reversal of STIM1 puncta is observed only under conditions when STIM1 is overexpressed alone; when both Orai1 and STIM1 proteins are co-expressed, the puncta are unaffected by 2-APB (18, 25). One possibility is that functional STIM1-Orai coupling is, in fact, interrupted by 2-APB under these conditions also but cannot be detected by optical methods. Therefore, in an alternative approach, we tested whether 2-APB changes the functional features of Orai3 channels that depend on STIM1 such as fast inactivation, potentiation, and the slow kinetics of direct activation.

As noted above, pronounced fast inactivation is a characteristic hallmark of store-operated CRAC channels and arises because of feedback inhibition of channel activity by the high local $[Ca^{2+}]_i$ around individual CRAC channels (36–38). In the presence of high doses of 2-APB, however, fast inactivation of Orai3 I_{CRAC} was completely eliminated (Fig. 8, *A* and *C*). In the example shown in Fig. 8*A*, 50 μM 2-APB caused delayed activation of the outward current over tens of seconds as described earlier. Over this duration, the extent of inactivation during brief voltage pulses to −100 mV declined, and inactivation was eventually completely eliminated. Interestingly, the removal of fast activation and current activation by 2-APB occurred at very different rates: the half-time for the removal of fast inactivation was less than the pulse interval (1 s) in all cells tested, considerably faster than the half-time for direct activation measured in the same cells (30 ± 4 s; $n =$ 5 cells). This result suggests that the molecular change ac-

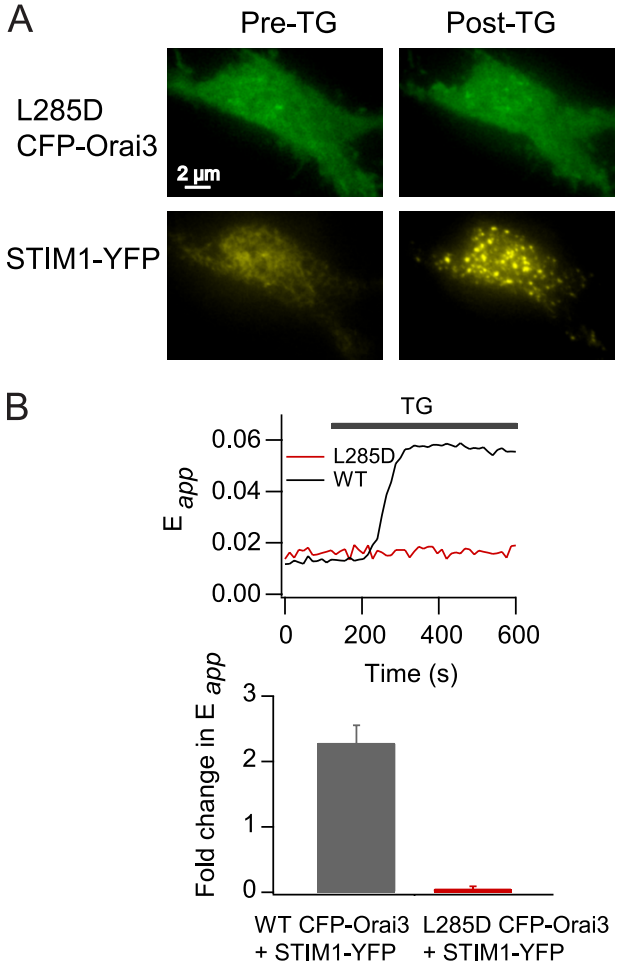

FIGURE 6. **L285D Orai3 mutation disrupts Orai3 interaction with STIM1.** *A*, a cell overexpressing L285D Orai3-CFP and STIM1-YFP was imaged using TIRF microscopy at rest and 15 min following exposure to 1 μM TG. Store depletion results in redistribution of STIM1-YFP into peripheral puncta, but the localization of L285D Orai3 is unchanged. *B*, the L285D mutation eliminates interaction with STIM1. The trace shows epifluorescence E-FRET in a cell co-expressing L285D Orai3 and STIM1-YFP. The bar graph *below* summarizes the -fold change in E_{app} following store depletion with 1 μM TG in WT CFP-Orai3 ($n = 54$ cells) and L285D CFP-Orai3 ($n = 10$ cells) cells co-expressing STIM1-YFP. E_{app} was averaged from five time lapse images at rest and five images taken 420 s following exposure to 1 μM TG.

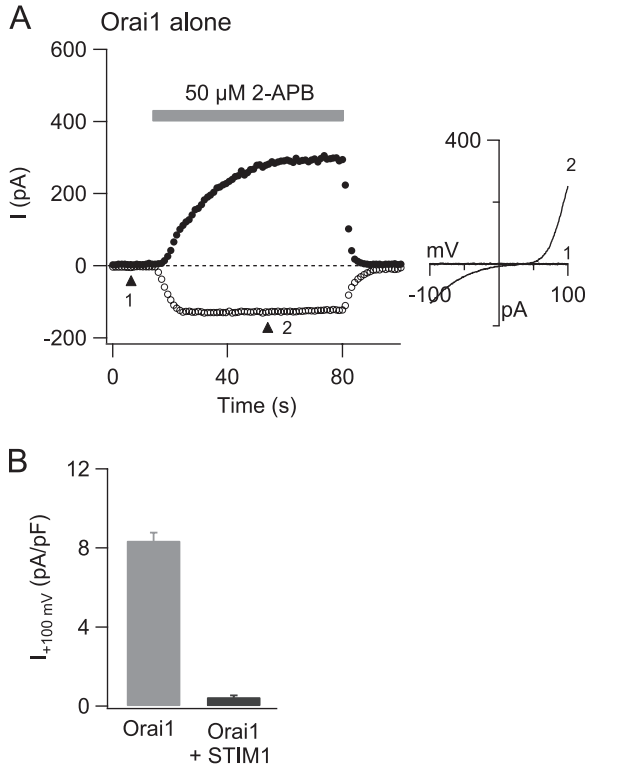

FIGURE 7. **STIM1 inhibits direct activation of Orai1 by high doses of 2-APB.** *A*, a cell overexpressing Orai1 alone was exposed to 50 μM 2-APB. Currents at −100 mV (*open circles*) and +100 mV (*closed circles*) from ramp I-Vs are plotted against time. The *right* plot shows the ramp I-V of the 2-APB-stimulated Orai1 current at the time points indicated by the *arrowheads*. Similar results were seen in seven of seven cells. *B*, summary of STIM1 inhibition on 2-APB activation of Orai1 current. The outward current density at +100 mV stimulated by 50 μM 2-APB was measured in cells overexpressing Orai1 alone or together with STIM1. In contrast to cells expressing Orai1 alone, outward currents were largely absent in cells co-expressing Orai1 and STIM1. *pF*, picofarad.

companying the removal of fast inactivation precedes the direct activation of Orai3 current.

Given that high concentrations of 2-APB reduce the Ca^{2+} permeability of Orai3 channels, one simple possibility is that the observed loss of fast inactivation arises due to a lower level of Ca^{2+} flux and corresponding increase in Na^+ flux through Orai3 channels. This seems unlikely, however, because applications of 2-APB (50 μM) in isotonic Ca^{2+} solutions (110 mM) with no Na^+ present also showed complete loss of Orai3 fast inactivation (Fig. 8, *B* and *C*). Because STIM1 is essential both for store-operated gating and for fast inactivation (32–34), the loss of fast inactivation in cells co-expressing Orai3 and STIM1 is consistent with uncoupling of STIM1 from Orai3 channels. Moreover, the distinct kinetics of the removal of fast inactivation and 2-APB activation suggests that STIM1 uncoupling occurs prior to 2-APB activation of the non-selective conductance.

Second, we examined whether STIM1-dependent potentiation by a low dose of 2-APB is affected following inhibition of the store-operated Orai3 conductance. For this, we compared the increase in current due to potentiation before and following inhibition of the store-operated conductance by 50 μM 2-APB. This comparison indicated that potentiation by a low dose of 2-APB (10 μM) is significantly reduced following inhibition of the store-operated current by 50 μM 2-APB (Fig. 8*D*). Because potentiation was dependent on STIM1 coupling (Fig. 1, *C* and *D*), the abrogation of potentiation following exposure to high doses of 2-APB is consistent with the hypothesis that high doses of 2-APB functionally uncouple STIM1-Orai3 interactions.

Third, we examined whether the kinetics of direct activation is affected by high doses of 2-APB. Because store-independent activation of STIM1-bound Orai3 channels is significantly slower than that of STIM1-free channels (Fig. 5, *C* and *D*), uncoupling of STIM1 from Orai3 by high concentrations of 2-APB is predicted to accelerate the kinetics of direct activation during subsequent drug applications. We tested this possibility by exploiting the fact that 2-APB inhibition of the store-operated conductance persists long after the removal of the drug, whereas direct 2-APB activation is readily reversed upon drug washout. Therefore, a high dose of 2-APB (30 μM)

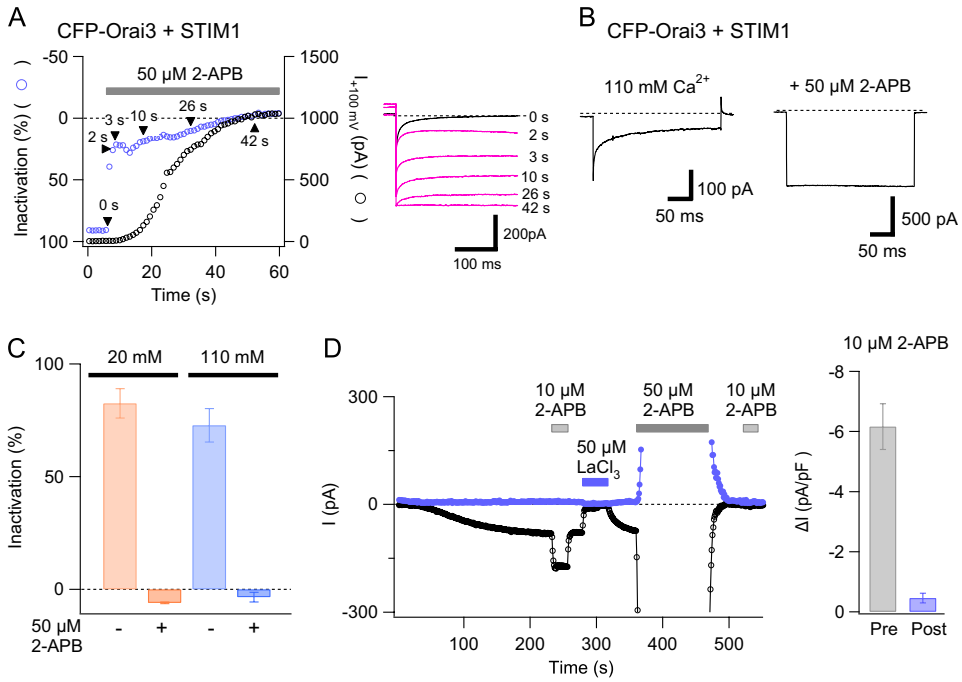

FIGURE 8. **High doses of 2-APB abolish fast inactivation and 2-APB-mediated potentiation of store-operated Orai3 currents.** *A*, a cell co-expressing CFP-Orai3 and STIM1 was treated with 1 μM TG to deplete intracellular Ca^{2+} stores prior to the recording. The cell was hyperpolarized to −100 mV (300 ms) at 1-s intervals to study fast inactivation during the application of a high dose of 2-APB (50 μM). The *left* graph plots the extent of inactivation and the amplitude of the outward current at +100 mV (obtained from ramps) in the same cell. Example traces at the time points indicated by the *arrowheads* are shown on the *right*. The extent of fast inactivation was quantified as $100 \times (1 - I_{ss}/I_{peak})$ where I_{peak} and I_{ss} are the currents at the start and end of a 300-ms voltage pulse to −100 mV. Following the complete removal of fast inactivation, the current exhibits time-dependent facilitation during the pulses, which causes the extent of inactivation value to become slightly negative. *B*, fast inactivation of the store-operated Orai3 I_{CRAC} in isotonic Ca^{2+} (110 mM) and in 50 μM 2-APB. The cell was transfected with STIM1 and CFP-Orai3. *C*, summary of the changes in fast inactivation by 50 μM 2-APB. *D*, potentiation is lost following inhibition of the store-operated Orai3 current. In a cell co-expressing STIM1 and CFP-Orai3, a low dose of 2-APB (10 μM) was applied prior to, and following inhibition of the store-operated Orai3 current by a high dose of 2-APB (50 μM). The y-axis is shown at a high gain to facilitate visualization of the store-operated Orai3 current. The bar graph on the *right* summarizes the degree of potentiation caused by 10 μM 2-APB before (*Pre*) and following (*Post*) inhibition of the store-operated current. *pF*, picofarad.

was applied to induce inhibition of the store-operated Orai3 current, then washed away, and reapplied following a delay of 2–3 min to study the behavior of direct activation (Fig. 9*A*). As expected, activation of Orai3 current during the first application of 2-APB occurred with a long delay (Fig. 9*A*). By contrast, the kinetics of activation of the non-selective current was significantly faster during the second 2-APB application with acceleration of both the latency and the rise time (Fig. 9, *B* and *C*). As a consequence, the behavior of the non-selective current in the second application of 2-APB strongly resembled the rapid activation seen in cells expressing Orai3 alone where the channels are likely to be free of STIM1. The most straightforward interpretation of this result is that 2-APB functionally uncouples STIM1 from Orai3 channels in the first application of the drug, resulting in abrogation of the store-operated conductance and promoting rapid 2-APB gating.

Acceleration of 2-APB Gating Is Directly Related to Inhibition of Store-operated Conductance—The findings presented above indicate that high doses of 2-APB functionally uncouple STIM1 from Orai3. Moreover, the data presented in Fig. 9, *A* and *B*, indicate that the STIM1-mediated inhibition of 2-APB activation of Orai3 channels is relieved following disengagement of STIM1 from Orai3. Thus, the ability of STIM1 to produce a long delay in 2-APB activation can be rationalized by supposing that STIM1 is required to first unbind from Orai3 channels before direct gating by 2-APB can occur. We investigated this possibility in two ways. First, we analyzed the relationship between the inhibition of the store-operated current and the latency of direct activation of the non-selective conductance during paired applications of 2-APB. We reasoned that if uncoupling of STIM1 is necessary for activation of the non-selective conductance, there should be correlation between the degree of inhibition of the store-operated conductance during the first exposure to 2-APB and the rate of direct activation in the second application of 2-APB. To vary the degree of inhibition of the store-operated conductance, we varied the duration of the drug exposure during the first application of 2-APB (50 μM). Consistent with this prediction, plots of the degree of inhibition of the store-operated current *versus* the rate of current activation (defined here as 1/latency) during the second application of 2-APB displayed a strong correlation (Fig. 9*D*), indicating that the antagonism to direct activation is relieved in direct proportion to the extent of STIM1 uncoupling. This result strongly suggests that 2-APB has to first uncouple STIM1 from Orai3 before direct activation can occur.

In a second related test, we examined whether manipulations that reduce 2-APB inhibition of the store-operated conductance also affect the kinetics of direct activation. As described earlier, 2-APB inhibition of the store-operated current is strongly reduced when the concentration of the permeant

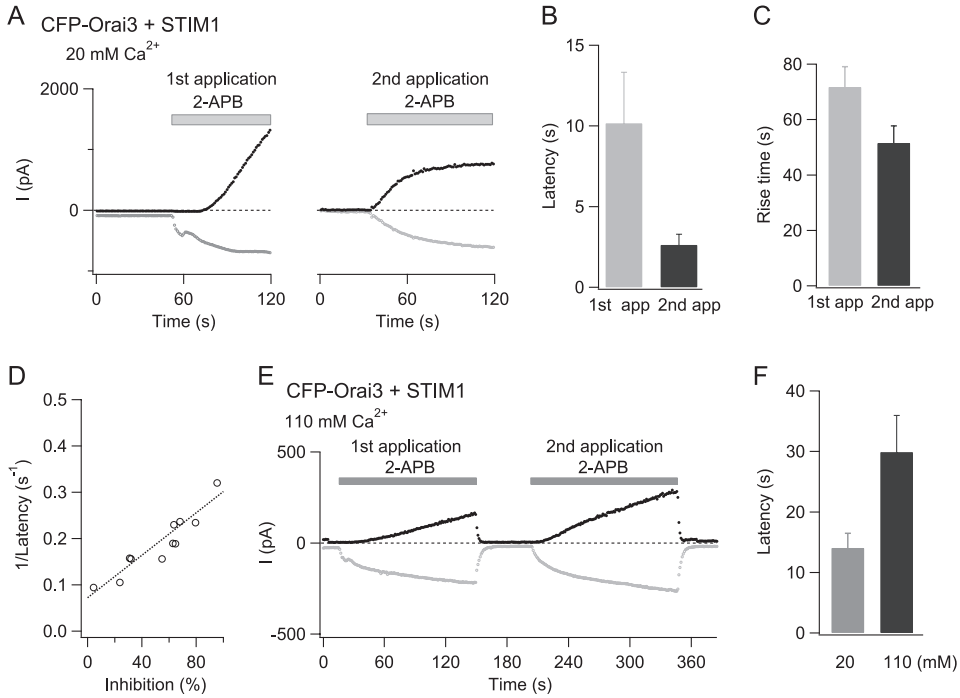

FIGURE 9. **2-APB inhibition of store-operated Orai3 current accelerates kinetics of direct activation.** *A*, an HEK293 cell overexpressing CFP-Orai3 and STIM1 was bathed in 1 μM TG to deplete stores and exposed to two applications of 2-APB (30 μM) separated by ~100 s. Currents at −100 (*gray* trace) and +100 mV (*black* trace) during each application are plotted against time. For clarity of the early activation kinetics, only the currents during the initial 60–80 s of 2-APB exposure are shown. In this cell, the initial 2-APB-stimulated current gradually inactivated over ~200 s following maximal activation, resulting in a smaller current during the second 2-APB application. *B*, summary of the latency of activation of the outward current at +100 mV during the first and second applications (*app*) of 30 μM 2-APB ($n = 4–6$ cells). *C*, summary of the 10–90% rise time of outward current activation during the first and second 2-APB applications ($n = 4$ cells). *D*, plot of inhibition of the store-operated Orai3 current at the end of the first pulse of 2-APB *versus* the rate of 2-APB-mediated outward current activation (1/latency) during the second drug application in single cells. The *dotted line* is a linear regression with a Pearson's coefficient of 0.95. *E*, currents activated by paired applications of 2-APB (50 μM) in 110 mM $Ca^{2+}{}_o$. *F*, summary of the latency of the outward current activation (at +100 mV) in 20 and 110 mM $Ca^{2+}{}_o$ during the first application of 2-APB.

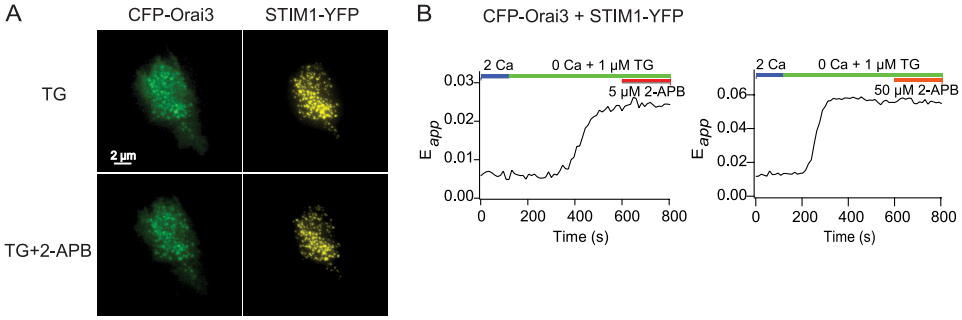

FIGURE 10. **High doses of 2-APB do not eliminate physical interactions between Orai3 and STIM1.** *A*, the store-depleted HEK293 cell shown in Fig. 4*A* was imaged using TIRF microscopy in the absence and presence of 2-APB. Application of 2-APB (50 μM) for 240 s did not visibly affect the punctate localization of CFP-Orai3 or STIM1-YFP. *B*, effects of low and high doses of 2-APB on STIM1-Orai3 FRET. Individual HEK293 cells co-expressing CFPOrai3 and STIM1-YFP were bathed in 1 μM TG to deplete ER Ca^{2+} stores and exposed to either 5 or 50 μM 2-APB. E-FRET was monitored using epifluorescence microscopy.

ion is raised to 110 mM Ca^{2+} (Fig. 2, *C* and *D*). If the rate of direct activation by 2-APB is related to the degree of inhibition of the store-operated current (uncoupling), then reduced inhibition of the store-operated current should be accompanied by a slower rate of direct activation. In agreement with this prediction, the latency of 2-APB activation during the second 2-APB application in 110 mM $Ca^{2+}{}_o$ was significantly longer than that seen in 20 mM $Ca^{2+}{}_o$ (Fig. 9*E*) (10.5 ± 1 s in 110 mM $Ca^{2+}{}_o$ *versus* 2.4 ± 0.3 s in 20 mM $Ca^{2+}{}_o$). What was particularly noteworthy was that the latency of current activation in the first application of 2-APB was also significantly longer in 110 mM $Ca^{2+}{}_o$ than in 20 mM $Ca^{2+}{}_o$ (Fig. 9, *E* and *F*). This result is expected if direct activation is related to the degree of STIM1 uncoupling and implies that uncoupling of STIM1 is a necessary prerequisite for the direct activation of the non-selective conductance by high doses of 2-APB.

2-APB Does Not Dissolve Orai3-STIM1 Puncta—Although the functional evidence presented above implies that 2-APB likely disrupts STIM1-Orai3 interactions, TIRF imaging revealed that this is not readily manifested as dissolution of STIM1-Orai3 puncta (Fig. 10*A*). Moreover, direct examination of STIM1-Orai3 interactions by FRET revealed that neither low nor high concentrations of 2-APB (5 and 50 μM) significantly diminished STIM1-Orai3 FRET. In fact, a low dose of 2-APB slightly enhanced Orai3-STIM1 FRET (5 ± 0.5% ($n = 18$; 5 μM 2-APB), reminiscent of previous findings with

STIM1 and Orai1 (18, 21, 25). Thus, the functional uncoupling of STIM1 and Orai3 is not accompanied by physical dissociation of the two proteins.

DISCUSSION

Complexity of 2-APB Effects on Orai3 Channels—In this study, we have found that 2-APB elicits many more effects on Orai3 currents than just the store-independent direct activation reported previously (17–20). Low doses of 2-APB (<10 μM) reversibly enhanced Orai3 I_{CRAC} without altering ion selectivity. Higher doses resulted in multiple effects, including strong suppression of the store-operated current, disappearance of fast inactivation, elimination of low dose potentiation, and store-independent activation with altered ion selectivity. 2-APB-mediated modulation of store-operated currents may have been overlooked in previous studies because the strong store-independent activation of Orai3 channels likely masked the other effects. The use of high concentrations of 2-APB (>50 μM), which accelerates the kinetics of direct activation, would have further exacerbated this problem. As a result, earlier studies emphasized the distinct behavior of Orai3 channels from the other Orai isoforms (17, 19, 39). However, here we found that the effects of 2-APB are qualitatively quite similar in Orai1 and Orai3 channels: in both subtypes, low doses of 2-APB potentiated channel activity, high doses inhibited the store-operated mode of activation and diminished fast inactivation, and in the absence of STIM1, both subtypes could be activated by high doses of 2-APB, although the latter effect was more robust in Orai3. These results strongly suggest that the molecular underpinnings of the 2-APB effects are conserved across these Orai isoforms.

Low Doses of 2-APB Potentiate Store-operated Orai3 Currents—Low doses of 2-APB boosted the activity of Orai3 CRAC channels once they were activated by store depletion. Several lines of evidence indicate that this mechanism of current enhancement differs from the direct activation caused by high 2-APB concentrations. First, potentiation at low concentrations occurred without changes in ion selectivity in contrast to the striking changes in Ca^{2+} and monovalent selectivity seen during direct activation. Second, Orai3 potentiation by low concentrations of 2-APB occurred only following depletion of Ca^{2+} stores and was largely absent in resting cells with replete ER Ca^{2+} stores. Third, potentiation required the presence of STIM1 and was absent in cells transfected with Orai3 alone and in cells in which STIM1 expression was silenced by siRNA (Fig. 1*D*). Likewise, potentiation was strongly diminished in an Orai3 mutant with impaired STIM1 binding (Fig. 5*B*). Thus, in contrast to the direct activation at high 2-APB concentrations, potentiation likely preferentially occurs on actively coupled channels and therefore differs mechanistically from direct activation, which results from the opening of closed channels.

FRET experiments indicated that low concentrations of 2-APB (5 μM) slightly enhanced Orai3-STIM1 FRET. This is reminiscent of increases in Orai1-STIM1 FRET and enhanced coupling between the C terminus of STIM1 and Orai1 produced by 2-APB (21, 25). Thus, as proposed previously (25), potentiation of Orai channels likely involves increased efficiency of channel coupling to STIM1. Such a mechanism is also supported by previous findings from noise analysis indicating that potentiation by low doses of 2-APB arises from the recruitment of CRAC channels from a silent state to one of high open probability, resembling the stepwise recruitment of closed channels following store depletion (40). Thus, both 2-APB-induced potentiation and the opening of CRAC channels by store depletion likely share common mechanisms involving increased binding of STIM1 with Orai channels.

A higher 2-APB concentration (50 μM) did not increase FRET between CFP-Orai3 and STIM1-YFP, in this respect differing from Orai1 channels, which exhibit increases in FRET at both low and high concentrations. We do not know the basis for the different behaviors of Orai3 and Orai1. A likely possibility is that potentiation and inhibition of CRAC channels by 2-APB could involve both association and dissociation of the STIM1-Orai complexes as described below.

High Doses of 2-APB Inhibit Store-operated Orai3 Gating—High concentrations of 2-APB (≥30 μM) inhibited store-operated gating and removed fast inactivation of Orai3 I_{CRAC}, reminiscent of 2-APB effects in native CRAC channels of immune cells and in Orai1 channels (4, 13, 17–19). Previous studies have suggested that inhibition of Orai1 currents by high doses of 2-APB occurs, at least in part, because of reversal of STIM1 puncta (17, 18, 39). However, as shown in other studies (18, 21, 25), we found that 50 μM 2-APB failed to detectably alter the localization of CFP-Orai3 and STIM1 when both proteins were co-expressed, suggesting that 2-APB inhibition under these conditions cannot be simply explained by reversal of STIM1 puncta. Nevertheless, at least three lines of evidence in the present study indicate that inhibitory doses of 2-APB functionally disrupt STIM1-Orai3 coupling. First, 2-APB eliminated fast inactivation in both Orai1 and Orai3 channels, a regulatory process that is known to require interaction of CRAC channels with STIM1 (32–34). In fact, in native CRAC channels of T-cells, the removal of fast inactivation occurs in parallel with the inhibition of the current (13) as would be expected if inhibition and the removal of fast inactivation both arise from functional decoupling of STIM1 from Orai1. Second, STIM1-dependent potentiation of Orai3 I_{CRAC} was strongly suppressed following inhibition of the store-operated Orai3 I_{CRAC}. Third, the kinetic behavior of direct activation was strongly accelerated following prior exposure to high concentrations of 2-APB such that 2-APB activation now closely resembled the behavior seen in cells expressing Orai3 alone or in a mutant of Orai3 (L285D) with impaired STIM1 binding. Collectively, these results argue that despite lack of direct evidence for a change in STIM-Orai binding, high concentrations of 2-APB functionally disengage STIM1 from Orai3.

One possibility that could reconcile the obvious lack of 2-APB effects on puncta with the apparent functional uncoupling of STIM1 and Orai3 suggested by the electrophysiological evidence is a scenario in which 2-APB affects different STIM1-binding sites on CRAC channels differentially. STIM1 reportedly binds to two distinct sites on Orai1, strongly to the C terminus and weakly to the N terminus (41, 42). Deletion of the Orai1 N terminus does not affect channel clustering or

STIM1-Orai1 FRET but precludes channel activation (41, 43, 44). By contrast, deletion or mutations in the C terminus abrogate STIM1 binding, punctum formation, and channel activation (43, 44). Thus, one possibility is that 2-APB either competitively or allosterically displaces STIM1 from the N terminus of Orai channels, thereby inhibiting store-operated gating without interrupting tight STIM1 binding at the C terminus. In effect, inhibition by 2-APB may be analogous to the defects of N-terminal Orai1 deletion mutations, which manifest no channel activity yet retain clustering and high levels of FRET between STIM1 and Orai1 (44).

STIM1 Antagonizes Direct Gating of Orai3 (and Orai1) Channels by 2-APB—A surprising finding was that overexpression of STIM1 dramatically slowed the direct activation of Orai3 channels by 2-APB in store-depleted cells. This was manifested both as a long delay in activation and, once activated, a longer rise time of the amplitude of the non-selective Orai3 current. An Orai3 mutant with diminished STIM1 binding did not exhibit this effect, indicating that interactions with STIM1 are required for the dampening of Orai3 activation. The inhibitory effects of STIM1 on the kinetics of 2-APB activation could be overcome by uncoupling STIM1 from Orai3 channels. Thus, these findings indicate that CRAC channels bound to STIM1 are resistant to store-independent gating by 2-APB. In Orai1 channels, the STIM1-mediated inhibition of direct activation appears even more robust: although high doses of 2-APB produced outwardly rectifying currents in all cells overexpressing Orai1 alone, this was not detected in cells co-expressing STIM1 and Orai1. Thus, there appears to be a reciprocal relationship between STIM1 gating and 2-APB gating of CRAC channels: STIM1 antagonizes the ability of 2-APB to directly activate Orai3 and Orai1 channels, whereas 2-APB suppresses the store-operated mode of activation by suppressing the ability of STIM1 to gate CRAC channels. Whether this type of reciprocal regulation has a physiological correlate is unclear. A recent study has reported that Orai1 channels in breast cancer-derived cells can be activated independently of ER Ca^{2+} stores and STIM1 by the Golgi Ca^{2+}-ATPase SPCA2 (22). Thus, the finding that CRAC channel activation can be invoked by multiple mechanisms raises the possibility that mutual antagonism as described here for STIM1 and 2-APB may be a general mechanism for cells to adjust CRAC channel activity depending on the nature of the upstream activation signal.

The inhibition of direct activation by STIM1 described above is reminiscent of the models that have been described for G protein inhibition of voltage-gated Ca^{2+} channels (45, 46). G$\beta\gamma$ subunits bind and inhibit voltage-activated Ca_V2 currents by stabilizing "reluctant gating" conformations of the channels. Once the G protein unbinds, the channel returns to a "willing gating" conformation where activation occurs normally (45). Likewise, STIM1-bound CRAC channels may occupy a functionally analogous reluctant state in which they are resistant to direct agonists such as 2-APB with direct gating only occurring following unbinding of STIM1.

What does the long delay in 2-APB gating mean in physical terms? A previous study has proposed that functional CRAC channels are formed by STIM1-mediated assembly of Orai1 dimers to yield tetrameric channels (8). This model suggests that in cells devoid of STIM1 the 2-APB-activated currents arise from Orai3 dimers. In the present study, our results imply that STIM1 has to be functionally uncoupled from STIM1-bound Orai3 channels before 2-APB activation can occur. Thus, one possibility is that the delay reflects the transition from Orai3 tetramers to dimers following uncoupling of STIM1. The dimeric Orai1 model, however, remains controversial, and other studies have reported that CRAC channels are tetramers of Orai1 both in STIM1-free and STIM1-bound states (9, 47). Thus, more studies are needed to clarify the precise subunit stoichiometry of the 2-APB-activated current.

The ability of 2-APB to directly gate a non-selective Orai3 conductance has raised hopes that this effect could be used to detect functional expression of Orai3 channels in native tissues (48). Indeed, a recent study has exploited this effect to demonstrate store-operated Ca^{2+} entry mediated by Orai3 channels in breast cancer cells (49). Nevertheless, the finding that STIM1 can suppress direct gating by 2-APB suggests that this approach may, at least in some cases, yield negative results even when Orai3 is functionally expressed. Although 2-APB is indeed able to overcome STIM1 inhibition and activate overexpressed Orai3 channels during prolonged 2-APB applications, this may not necessarily occur at physiological levels of STIM1 and Orai3 expression, potentially explaining the paucity of reports demonstrating 2-APB activation of Orai3 channels in native tissues.

Acknowledgments—We thank members of the laboratory for stimulating discussions and Anita Engh, Jack Waters, Stefan Feske, and Tara Hornell for comments on the manuscript.

REFERENCES

1. Putney, J. W. (2009) *Immunol. Rev.* **231,** 10–22
2. Parekh, A. B. (2010) *Nat. Rev. Drug Discov.* **9,** 399–410
3. Hogan, P. G., Lewis, R. S., and Rao, A. (2010) *Annu. Rev. Immunol.* **28,** 491–533
4. Feske, S., Gwack, Y., Prakriya, M., Srikanth, S., Puppel, S. H., Tanasa, B., Hogan, P. G., Lewis, R. S., Daly, M., and Rao, A. (2006) *Nature* **441,** 179–185
5. Zhang, S. L., Yeromin, A. V., Zhang, X. H., Yu, Y., Safrina, O., Penna, A., Roos, J., Stauderman, K. A., and Cahalan, M. D. (2006) *Proc. Natl. Acad. Sci. U.S.A.* **103,** 9357–9362
6. Vig, M., Peinelt, C., Beck, A., Koomoa, D. L., Rabah, D., Koblan-Huberson, M., Kraft, S., Turner, H., Fleig, A., Penner, R., and Kinet, J. P. (2006) *Science* **312,** 1220–1223
7. Mignen, O., Thompson, J. L., and Shuttleworth, T. J. (2008) *J. Physiol.* **586,** 419–425
8. Penna, A., Demuro, A., Yeromin, A. V., Zhang, S. L., Safrina, O., Parker, I., and Cahalan, M. D. (2008) *Nature* **456,** 116–120
9. Ji, W., Xu, P., Li, Z., Lu, J., Liu, L., Zhan, Y., Chen, Y., Hille, B., Xu, T., and Chen, L. (2008) *Proc. Natl. Acad. Sci. U.S.A.* **105,** 13668–13673
10. Feske, S. (2009) *Immunol. Rev.* **231,** 189–209
11. Feske, S. (2010) *Pflugers Arch.* **460,** 417–435
12. Bootman, M. D., Collins, T. J., Mackenzie, L., Roderick, H. L., Berridge, M. J., and Peppiatt, C. M. (2002) *FASEB J.* **16,** 1145–1150
13. Prakriya, M., and Lewis, R. S. (2001) *J. Physiol.* **536,** 3–19
14. Ma, H. T., Venkatachalam, K., Parys, J. B., and Gill, D. L. (2002) *J. Biol. Chem.* **277,** 6915–6922
15. Lis, A., Peinelt, C., Beck, A., Parvez, S., Monteilh-Zoller, M., Fleig, A., and Penner, R. (2007) *Curr. Biol.* **17,** 794–800

16. DeHaven, W. I., Smyth, J. T., Boyles, R. R., and Putney, J. W., Jr. (2007) *J. Biol. Chem.* **282,** 17548–17556
17. Peinelt, C., Lis, A., Beck, A., Fleig, A., and Penner, R. (2008) *J. Physiol.* **586,** 3061–3073
18. DeHaven, W. I., Smyth, J. T., Boyles, R. R., Bird, G. S., and Putney, J. W., Jr. (2008) *J. Biol. Chem.* **283,** 19265–19273
19. Zhang, S. L., Kozak, J. A., Jiang, W., Yeromin, A. V., Chen, J., Yu, Y., Penna, A., Shen, W., Chi, V., and Cahalan, M. D. (2008) *J. Biol. Chem.* **283,** 17662–17671
20. Schindl, R., Bergsmann, J., Frischauf, I., Derler, I., Fahrner, M., Muik, M., Fritsch, R., Groschner, K., and Romanin, C. (2008) *J. Biol. Chem.* **283,** 20261–20267
21. Wang, Y., Deng, X., Zhou, Y., Hendron, E., Mancarella, S., Ritchie, M. F., Tang, X. D., Baba, Y., Kurosaki, T., Mori, Y., Soboloff, J., and Gill, D. L. (2009) *Proc. Natl. Acad. Sci. U.S.A.* **106,** 7391–7396
22. Feng, M., Grice, D. M., Faddy, H. M., Nguyen, N., Leitch, S., Wang, Y., Muend, S., Kenny, P. A., Sukumar, S., Roberts-Thomson, S. J., Monteith, G. R., and Rao, R. (2010) *Cell* **143,** 84–98
23. Yamashita, M., Navarro-Borelly, L., McNally, B. A., and Prakriya, M. (2007) *J. Gen. Physiol.* **130,** 525–540
24. Prakriya, M., Feske, S., Gwack, Y., Srikanth, S., Rao, A., and Hogan, P. G. (2006) *Nature* **443,** 230–233
25. Navarro-Borelly, L., Somasundaram, A., Yamashita, M., Ren, D., Miller, R. J., and Prakriya, M. (2008) *J. Physiol.* **586,** 5383–5401
26. Zal, T., and Gascoigne, N. R. (2004) *Biophys. J.* **86,** 3923–3939
27. Luik, R. M., Wu, M. M., Buchanan, J., and Lewis, R. S. (2006) *J. Cell Biol.* **174,** 815–825
28. Xu, P., Lu, J., Li, Z., Yu, X., Chen, L., and Xu, T. (2006) *Biochem. Biophys. Res. Commun.* **350,** 969–976
29. Wu, M. M., Luik, R. M., and Lewis, R. S. (2007) *Cell Calcium* **42,** 163–172
30. Frischauf, I., Muik, M., Derler, I., Bergsmann, J., Fahrner, M., Schindl, R., Groschner, K., and Romanin, C. (2009) *J. Biol. Chem.* **284,** 21696–21706
31. Covington, E. D., Wu, M. M., and Lewis, R. S. (2010) *Mol. Biol. Cell* **21,** 1897–1907
32. Mullins, F. M., Park, C. Y., Dolmetsch, R. E., and Lewis, R. S. (2009) *Proc. Natl. Acad. Sci. U.S.A.* **106,** 15495–15500
33. Derler, I., Fahrner, M., Muik, M., Lackner, B., Schindl, R., Groschner, K., and Romanin, C. (2009) *J. Biol. Chem.* **284,** 24933–24938
34. Lee, K. P., Yuan, J. P., Zeng, W., So, I., Worley, P. F., and Muallem, S. (2009) *Proc. Natl. Acad. Sci. U.S.A.* **106,** 14687–14692
35. Fahrner, M., Muik, M., Derler, I., Schindl, R., Fritsch, R., Frischauf, I., and Romanin, C. (2009) *Immunol. Rev.* **231,** 99–112
36. Zweifach, A., and Lewis, R. S. (1995) *J. Gen. Physiol.* **105,** 209–226
37. Fierro, L., and Parekh, A. B. (1999) *J. Membr. Biol.* **168,** 9–17
38. Hoth, M., and Penner, R. (1992) *Nature* **355,** 353–356
39. Goto, J., Suzuki, A. Z., Ozaki, S., Matsumoto, N., Nakamura, T., Ebisui, E., Fleig, A., Penner, R., and Mikoshiba, K. (2010) *Cell Calcium* **47,** 1–10
40. Prakriya, M., and Lewis, R. S. (2006) *J. Gen. Physiol.* **128,** 373–386
41. Park, C. Y., Hoover, P. J., Mullins, F. M., Bachhawat, P., Covington, E. D., Raunser, S., Walz, T., Garcia, K. C., Dolmetsch, R. E., and Lewis, R. S. (2009) *Cell* **136,** 876–890
42. Zhou, Y., Meraner, P., Kwon, H. T., Machnes, D., Oh-hora, M., Zimmer, J., Huang, Y., Stura, A., Rao, A., and Hogan, P. G. (2010) *Nat. Struct. Mol. Biol.* **17,** 112–116
43. Li, Z., Lu, J., Xu, P., Xie, X., Chen, L., and Xu, T. (2007) *J. Biol. Chem.* **282,** 29448–29456
44. Muik, M., Frischauf, I., Derler, I., Fahrner, M., Bergsmann, J., Eder, P., Schindl, R., Hesch, C., Polzinger, B., Fritsch, R., Kahr, H., Madl, J., Gruber, H., Groschner, K., and Romanin, C. (2008) *J. Biol. Chem.* **283,** 8014–8022
45. Boland, L. M., and Bean, B. P. (1993) *J. Neurosci.* **13,** 516–533
46. Ikeda, S. R., and Dunlap, K. (1999) *Adv. Second Messenger Phosphoprotein Res.* **33,** 131–151
47. Madl, J., Weghuber, J., Fritsch, R., Derler, I., Fahrner, M., Frischauf, I., Lackner, B., Romanin, C., and Schütz, G. J. (2010) *J. Biol. Chem.* **285,** 41135–41142
48. Putney, J. W. (2010) *Mol. Interv.* **10,** 209–218
49. Motiani, R. K., Abdullaev, I. F., and Trebak, M. (2010) *J. Biol. Chem.* **285,** 19173–19183